Rapid Translocation of Zn^{2+} From Presynaptic Terminals Into Postsynaptic Hippocampal Neurons After Physiological Stimulation

YANG LI,[1] CHRISTOPHER J. HOUGH,[2] SANG WON SUH,[3] JOHN M. SARVEY,[1] AND CHRISTOPHER J. FREDERICKSON[3,4]

[1]*Department of Pharmacology and* [2]*Department of Psychiatry, Uniformed Services University of the Health Sciences, Bethesda, Maryland 20814;* [3]*Center for Biomedical Engineering and Department of Anatomy and Neuroscience, University of Texas Medical Branch; and* [4]*NeuroBioTex, Inc., Galveston, Texas 77555*

Received 29 December 2000; accepted in final form 25 May 2001

Li, Yang, Christopher J. Hough, Sang Won Suh, John M. Sarvey, and Christopher J. Frederickson. Rapid translocation of Zn^{2+} from presynaptic terminals into postsynaptic hippocampal neurons after physiological stimulation. *J Neurophysiol* 86: 2597–2604, 2001. Zn^{2+} is found in glutamatergic nerve terminals throughout the mammalian forebrain and has diverse extracellular and intracellular actions. The anatomical location and possible synaptic signaling role for this cation have led to the hypothesis that Zn^{2+} is released from presynaptic boutons, traverses the synaptic cleft, and enters postsynaptic neurons. However, these events have not been directly observed or characterized. Here we show, using microfluorescence imaging in rat hippocampal slices, that brief trains of electrical stimulation of mossy fibers caused immediate release of Zn^{2+} from synaptic terminals into the extracellular microenvironment. Release was induced across a broad range of stimulus intensities and frequencies, including those likely to induce long-term potentiation. The amount of Zn^{2+} release was dependent on stimulation frequency (1–200 Hz) and intensity. Release of Zn^{2+} required sodium-dependent action potentials and was dependent on extracellular Ca^{2+}. Once released, Zn^{2+} crosses the synaptic cleft and enters postsynaptic neurons, producing increases in intracellular Zn^{2+} concentration. These results indicate that, like a neurotransmitter, Zn^{2+} is stored in synaptic vesicles and is released into the synaptic cleft. However, unlike conventional transmitters, it also enters postsynaptic neurons, where it may have manifold physiological functions as an intracellular second messenger.

INTRODUCTION

Histochemically reactive, ionic zinc (Zn^{2+}) is found in a specific subset of glutamatergic nerve terminals throughout the mammalian cortex and limbic region and is especially abundant in the mossy fiber axons of the hippocampal formation (Frederickson et al. 2000). Ultrastructural studies show that most of the Zn^{2+} detected by histochemical stains is localized within synaptic vesicles of glutamatergic neurons (Frederickson et al. 1983; Haug 1967; Perez-Clausell and Danscher 1985). Zn^{2+} is a potent modulator of amino acid receptors. Its actions include the inhibition of *N*-methyl-D-aspartate (NMDA) receptors and potentiation of AMPA receptors (Peters et al. 1987; Westbrook and Mayer 1987). Zn^{2+} can penetrate ligand-gated channels such as NMDA receptors, Ca^{2+}-permeable AMPA/kainate receptors, and voltage-dependent Ca^{2+} channels (VDCC) in postsynaptic neurons (Koh and Choi 1994; Sensi et al. 1999; Weiss and Sensi 2000), where it can directly influence various signaling cascades (Brewer et al. 1979; Hubbard et al. 1991; Park and Koh 1999). Although these effects have been observed only in dissociated cells with exogenously added Zn^{2+}, it has been speculated for many years that endogenous Zn^{2+} may act as a neurotransmitter or neuromodulator at excitatory synapses.

It has been surmised for some time that Zn^{2+} is released from synaptic terminals by a variety of stimuli. This conclusion was based on the localization of vesicular Zn^{2+} in synaptic terminals and on indirect observations of loss of Zn^{2+} from synaptic terminals following depolarizing stimuli (Aniksztejn et al. 1987; Assaf and Chung 1984; Howell et al. 1984; Perez-Clausell and Danscher 1986). Because Zn^{2+} may have a critical function in synaptic transmission, we felt that it was necessary to directly observe Zn^{2+} release to confirm this hypothesis. By doing so, we would be able to characterize Zn^{2+} release and compare it with the release of neurotransmitters from the synaptic terminals to understand the function of Zn^{2+} in the CNS.

The high concentrations of Zn^{2+} in the hippocampal mossy fiber pathway make it an attractive system for characterizing synaptically released Zn^{2+} (Frederickson et al. 2000). In this study, we loaded and perfused hippocampal slices with the newly introduced Zn^{2+}-selective fluorescent probe Newport Green (NG) (Haugland 1996) to image extracellular and intracellular Zn^{2+}. We have found that electrical stimulation of mossy fibers induces fast Zn^{2+} release from mossy fiber terminals. Characterization of this release has revealed that, like neurotransmitter release, Zn^{2+} release requires sodium-dependent action potentials and extracellular Ca^{2+}. Furthermore, we observed a rapid increase of intracellular Zn^{2+} in postsynaptic neurons after electrical stimulation, indicating synaptic translocation of the released Zn^{2+} into postsynaptic neurons.

METHODS

Preparation of hippocampal slices and electrical stimulation

Experiments were conducted according to the principles set forth in the "Guide for Care and Use of Laboratory Animals," Institute of

Address for reprint requests: J. Sarvey, Dept. of Pharmacology, Uniformed Services University of the Health Sciences, 4301 Jones Bridge Rd., Bethesda, MD 20814 (E-mail: jsarvey@usuhs.mil).

The costs of publication of this article were defrayed in part by the payment of page charges. The article must therefore be hereby marked "*advertisement*" in accordance with 18 U.S.C. Section 1734 solely to indicate this fact.

Animal Resources, National Research Council, National Institutes of Health Publication No. 74-23. Transverse 200–300 μm hippocampal slices from male adult Sprague-Dawley rats were prepared according to the standard procedure (Sarvey et al. 1989) and then kept in an incubation chamber at room temperature for at least 1 h prior to imaging experiments. Slices were bathed in the artificial cerebrospinal fluid (ACSF) with the composition (in mM) of 124 NaCl, 1.75 KCl, 1.3 $MgSO_4$, 2.4 $CaCl_2$, 1.25 KH_2PO_4, 26 $NaHCO_3$, and 10 dextrose continuously bubbled with 95% O_2-5% CO_2 (pH 7.4). Bipolar electrodes (75-μm-diam wire, 300–500 μm apart) were used for electrical stimulation. The stimulation electrodes were placed in the infragranular layer or hilar region of the dentate gyrus. Trains of orthodromic stimuli (200-μs pulses at 500 μA unless otherwise noted) of various frequencies were delivered using an S44 stimulator and model PS1U6 photoelectric stimulus isolation unit (Grass Electronics, Quincy, MA).

Zn^{2+} imaging

For extracellular Zn^{2+} fluorescence imaging, hippocampal slices were preloaded with 20 μM NG dipotassium salt at room temperature in the dark for at least 30 min, and recordings were made with NG dipotassium salt in the ACSF bathing the slice. For intracellular Zn^{2+} imaging, the slices were preloaded with 50 μM NG diacetate, 0.1% pluronic acid, and 0.5% dimethyl sulfoxide for 1 h. Then extracellular NG diacetate was washed out with ACSF. Because we were concerned that DMSO might affect membrane properties, we tested the electrophysiological responses of mossy fiber-CA3 pyramidal cell synapses in hippocampal slices treated for 1 h with 0.5% DMSO and 0.1% pluronic acid. These slices demonstrated comparable physiological membrane properties, i.e., population excitatory postsynaptic potential (EPSP), spike, and robust paired-pulse facilitation of the EPSP, as with slices in normal ACSF. The stimulation intensities (at 30-μs duration) used to evoke half-maximum EPSP and spike were 100 ± 16 and 250 ± 44 (SE) μA ($n = 5$), respectively, for slices in normal ACSF, and 110 ± 19 and 240 ± 36 μA ($n = 5$), respectively, for slices in ACSF containing DMSO and pluronic acid. All experiments were performed at 32°C under constant ACSF perfusion on the thermostatically heated stage of an inverted microscope (Zeiss Axiovert 140, Oberkochen, Germany) coupled to a Xenon light source and monochromator set to 506 nM. Background fluorescence (autofluorescence) was not subtracted because it was below the detection limit of our camera. Emitted light images at 533 nm or greater were acquired through a 10 × 0.1 NA objective with an intensified CCD camera (PTI model IC-100) and digitized using ImageMaster software (PTI, Manmouth Junction, NJ).

Sensitivity of NG to Zn^{2+}

In control experiments performed without slices, we tested the ability of NG to measure physiologically relevant concentrations of Zn^{2+} in ACSF. The testing buffer was made with *puriss* grade salts (Fluka Chemical, Ronkonkoma, NY) in double deionized water, which was then further stripped of divalent metal ions by passage over Chelex-100 columns (Bio-Rad, Richmond, CA), and stored in plastic containers. $ZnCl_2$ was added to divalent cation-free ACSF containing 1.0 μM NG dipotassium salt and equilibrated with 95% O_2-5% CO_2 (pH 7.4). Fluorescence intensity increased with increasing Zn^{2+} concentration between 100 nM and 300 μM. Using the equation $F = F_{max} \cdot L^n/(K_d + L^n)$, where F_{max} is the fluorescence at dye saturation, L is the concentration of Zn^{2+}, K_d is the equilibrium dissociation constant, and n is the Hill coefficient, we found our data fit the equation (sum of squared differences = 1.59 ± 0.01) when F_{max} = 14.3 units, $K_d = 3.26$ μM and $n = 0.976$. The K_d is threefold greater than that obtained by others in a MOPS (3-[*N*-morpholino]propanesulfonic acid) buffer (1.0) (Haugland 1996). This difference is not due to the presence of Ca^{2+} and Mg^{2+} because the detection of Zn^{2+} by NG fluorescence was minimally affected by the presence of Ca^{2+} and Mg^{2+} at physiological concentrations (Fig. 1). Ca^{2+} or Mg^{2+} (up to 1 mM), in the absence of Zn^{2+}, had little effect on the dye fluorescence emission, which is consistent with previous reports (Canzoniero et al. 1999; Haugland 1996).

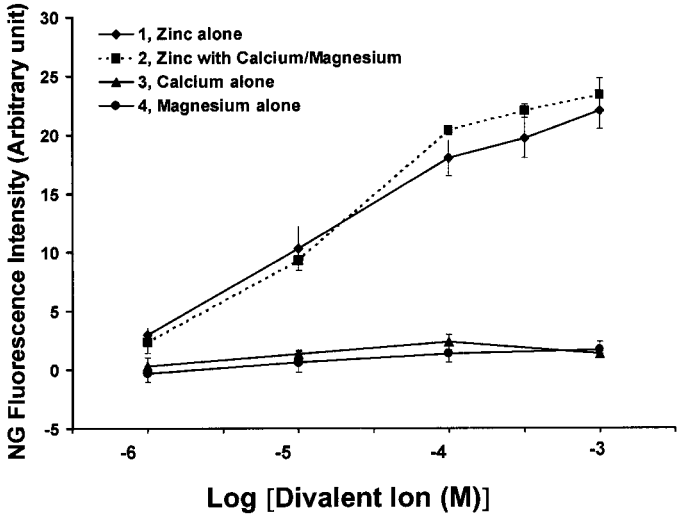

FIG. 1. Selectivity of Newport Green (NG) fluorescence for Zn^{2+} in the presence of a high concentration of Ca^{2+} and Mg^{2+}. Log concentration-response curves of NG to Zn^{2+} and 2 other divalent ions, Ca^{2+} and Mg^{2+}, that are found in artificial cerebrospinal fluid (ACSF). Changes of NG fluorescence intensity to Zn^{2+} (Curve 1, 2) were minimally affected by the presence of physiological levels of Ca^{2+} (2.4 mM) and Mg^{2+} (1.3 mM). Ca^{2+} or Mg^{2+}, in the absence of Zn^{2+} (curves 3 and 4), produced barely detectable changes in NG fluorescence. Values plotted are the means ± SE, $n = 3$ in each curve.

Determination of Zn^{2+} concentration

Zn^{2+} concentrations were calculated using the formula described by Grynkiewicz et al. (1985): $[Zn^{2+}] = K_d (F - F_{min})/(F_{max} - F)$, where F is the measured fluorescence intensity. F_{max} and F_{min} were obtained by measuring the dye fluorescence in the presence of 1 mM $ZnCl_2$ added to the ACSF bathing the slice, removing the Zn^{2+} by perfusing with Zn^{2+}-free ACSF, and then measuring the dye fluorescence again during perfusion with Zn^{2+}-free ACSF plus 10 mM Ca-EDTA.

TSQ staining of Zn^{2+}

After being electrically stimulated and frozen, slices were sectioned at 20 μm. Sections were stained for Zn^{2+} with the histochemical reagent *N*-(6-methoxy-8-quinolyl)-*p*-toluenesulfonamide (TSQ) by immersion in a solution of TSQ (4.5 μM) in 140 mM sodium barbital and 140 mM sodium acetate buffer (pH 10.5–11) for 60 s according to Frederickson et al. (1987). Images were captured with an Olympus inverted microscope (excitation, 355–375 nm, dichroic beam splitter, 380 nm, barrier, 420 nm long-pass) with a 20 × 0.7 N. A. UplanApo objective by a Diagnostic Spot cooled megapixel CCD camera and Spot Image analysis system (Diagnostic Instruments).

Statistics

All measurements are given as means ± SE. Statistical significance was tested using the Student's *t*-test, and $P < 0.05$ considered significant.

Materials

NG and TSQ were obtained from Molecular Probes (Eugene, OR). Ethylenediaminetetraacetic acid disodium-calcium salt (CaEDTA) and tetrodotoxin (TTX) were obtained from Sigma (St. Louis, MO).

RESULTS

To detect the release of Zn^{2+} from nerve terminals, we used the Zn^{2+} selective fluorescent dye, NG. Because vesicular Zn^{2+} is concentrated in the giant axonal boutons of hippocampal mossy fibers, we focused on the hilar region of the dentate gyrus where these axons form synapses with dendrites of CA3 pyramidal cells and interneurons. With cell-impermeable NG in the ACSF bathing the slice, a brief stimulation (100 Hz, 0.2-ms pulses for 5 s) of the mossy fibers produced an immediate increase in fluorescence in the region of the slice along the efferent pathway of the stimulated mossy fibers (Fig. 2*A*). The onset of fluorescence was rapid and could be detected within the smallest interval of time (33 ms) permitted by our equipment (Fig. 2*B*). Basal extracellular Zn^{2+} concentrations in the hilar region of the dentate gyrus were estimated to be 1.8 ± 0.8 μM ($n = 4$), while a concentration of 11.7 ± 2.6 μM ($n = 4$) was observed during 5-s bursts of electrical stimulation at 100 Hz (see METHODS). A similar fluorescence increase could be obtained by perfusing the slice with a depolarizing concentration of KCl (25 mM, Fig. 2*C*), a well-established means of depolarizing membrane to cause release of transmitters. The fluorescence increase elicited by either electrical stimulation or 50 mM KCl could be blocked by the presence of CaEDTA, a cell-impermeable chelator of Zn^{2+} that does not appreciably reduce Ca^{2+} or Mg^{2+} concentrations (Wang and Quastel 1990; Westergaard et al. 1995) (Fig. 2*D*). These results suggest that

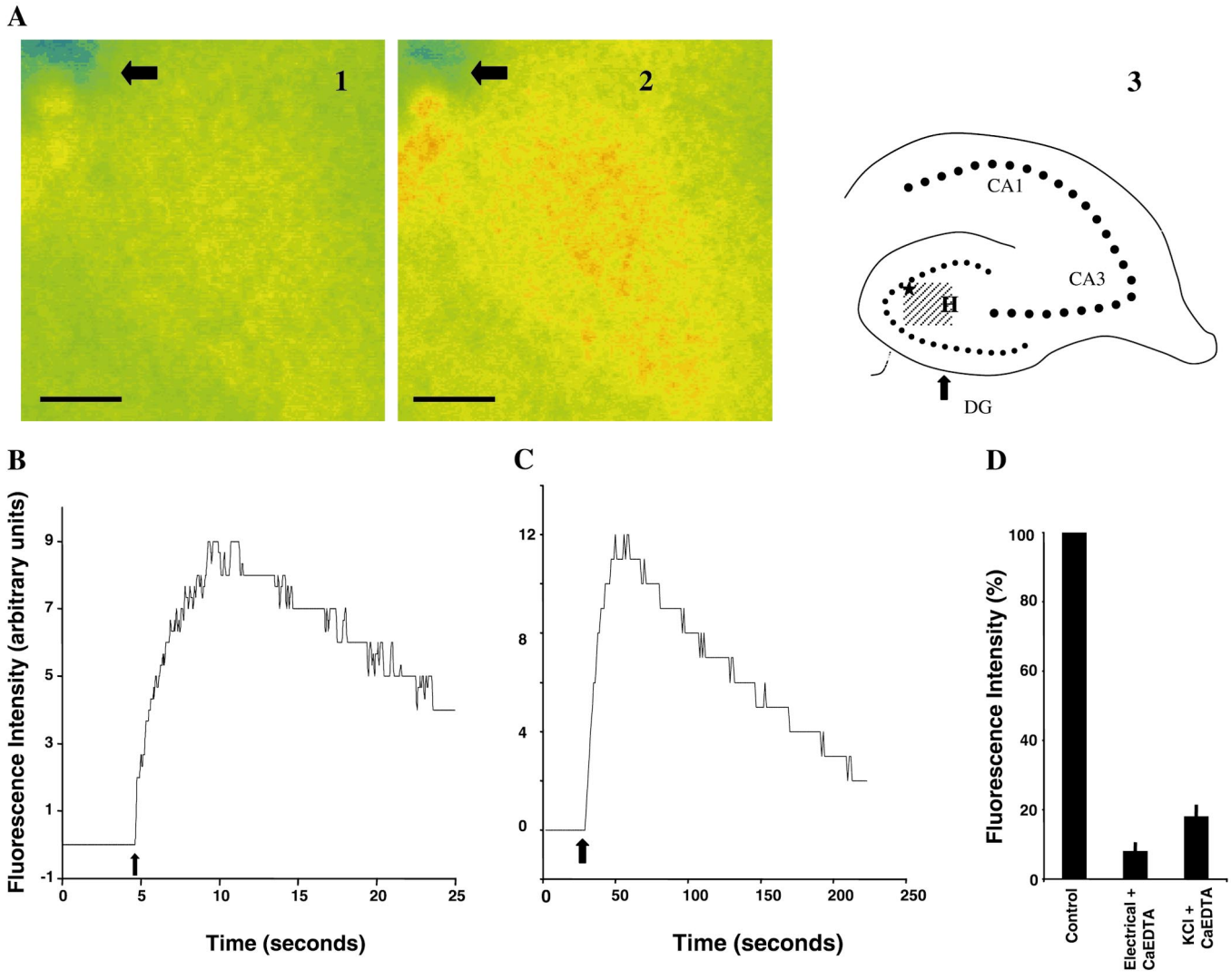

FIG. 2. Stimulation-induced release of Zn^{2+}. *A*: images of the hilus of hippocampal dentate gyrus perfused with 20 μM NG dipotassium salt before (*1*) and 0.5 s after (*2*) electrical stimulation (200 μs, 0.5-mA pulses at 100 Hz for 5 s). ← in *1* and *2*, placement of the stimulation electrodes. Scale bars are 100 μm. *A3*: hilus (H) of the hippocampus. ▨, region where images were acquired. ★, the placement of electrode. DG, dentate gyrus. *B*: electrical stimulation (100 Hz for 5 s) evoked rapid release of Zn^{2+} from neuronal terminals measured by changes in NG fluorescence intensity. ↑, the beginning of stimulation. *C*: KCl-induced release of Zn^{2+}. ↑, starting time of 25 mM KCl stimulus. *D*: electrical stimulation and KCl-evoked increase of NG fluorescence were blocked in the presence of 10 mM Ca-EDTA, a Zn^{2+} chelator. KCl concentration was 50 mM. Values plotted are the mean ± SE, $n = 3$; $P < 0.01$ in both conditions (statistical significance in all measurements was tested using the Student's *t*-test and $P < 0.05$ considered significant). The *y* axis value represents the fluorescence emission intensity of the dye/ion complex minus the fluorescence of the unstimulated slice.

Zn^{2+} can be released from nerve terminals by electrical stimulation or depolarization with KCl.

Four additional tests were undertaken to verify that the stimulation-induced fluorescence was due to physiological release of Zn^{2+} from presynaptic terminals. Specifically, we tested for release being confined to the axonal pathway being stimulated, dependent on stimulation intensity and frequency, sensitive to TTX, and dependent on extracellular Ca^{2+}.

Mossy fibers extend from dentate granule cells to the dendrites of hilar interneurons and CA3 pyramidal cells. In general, stimulation-induced Zn^{2+} release could be detected up to several hundred micrometers along the trajectory of the mossy fibers (from granule cells to CA3). As shown in three adjacent regions of interest (ROIs) in Fig. 3, *A* and *B*, the greatest fluorescence signal was always detected adjacent to the electrode, with lower signal amplitudes observed at greater distances, presumably due to the cutting of axons during preparation of the slices. We observed no perceptible delay in the onset of release in the ROIs along the mossy fiber projection. The fluorescence of the molecular layer, where the granule cell dendrites are located (adjacent to the electrodes but in a position outside the hilus, as shown in ROI4 in Fig. 3*A*), did not increase after stimulation. This result could not have occurred if the spread of Zn^{2+} release from the electrodes were transmitted by glial cells or neuronal dendrites.

If Zn^{2+} release were to occur during normal nerve transmission, one would not expect the conditions required to elicit this release by electrical stimulation to be extreme. Rather the degree of Zn^{2+} release should vary continuously with the degree of electrical stimulation from the lowest to highest practical frequencies. We found that electrically stimulated Zn^{2+} release was frequency dependent and could be detected with as little as 10-Hz stimulation at 500 μA (Fig. 3*C*). The degree of Zn^{2+} release also increased with increasing stimulus amplitudes ranging from 20 to 500 μA (100 Hz over 5 s; Fig. 3*D*).

The release of neurotransmitter during synaptic transmission requires the propagation of axonal action potentials to nerve terminals. TTX (2 μM), which blocks the sodium-dependent action potential, markedly reduced Zn^{2+} release by electrical

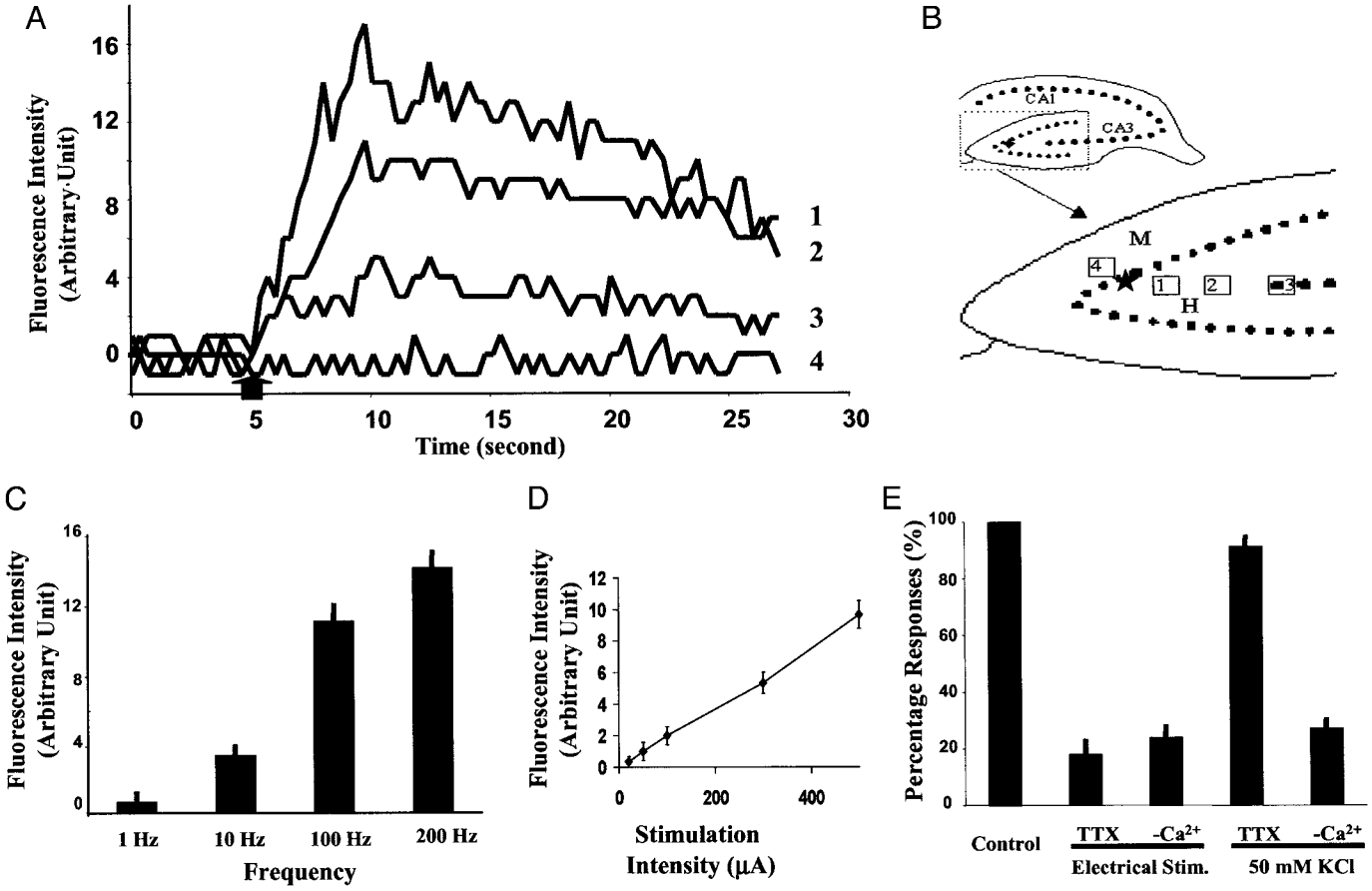

FIG. 3. Characteristics of Zn^{2+} release. *A*: electrical stimulation (100 Hz for 10 s) evoked release of Zn^{2+} from nerve terminals measured by change of fluorescence intensity. Changes of fluorescence with time at 4 separate regions of interest (ROIs) were plotted as curves 1, 2, 3, and 4. ↑, the beginning of stimulation. *B*: ROIs in DG. DG is enlarged from depiction of hippocampal slice, *top left*. Four □ represent ROIs, the number of which corresponds with that of the curve plotted in *A*. ⋆, the placement of electrode in the slice. H, hilus; M, molecular layer. *C*: Zn^{2+} release from synaptic terminals is stimulation frequency dependent. Each data point is the mean of 3 determinations. Error bars indicate SE. *D*: Zn^{2+} released by 100-Hz stimulation for 5 s increased with increasing stimulus intensity (μA). Each data point is the mean of 5 determinations. Error bars indicate SE. *E*: effects of TTX (2 μM), and withdrawal of Ca^{2+}($-Ca^{2+}$) on electrical stimulation and 50 mM potassium-induced release of Zn^{2+} from synaptic terminals. Each data bar is the mean of 5 determinations. Error bars indicate SE. *y* axis values of this figure represent the fluorescence emission intensity increases above basal as described in Fig. 2.

stimulation (Fig. 3*E*). On the other hand, TTX produced little effect on Zn^{2+} release evoked by a high concentration K^+ (Fig. 3*E*), which induces Ca^{2+} influx by directly depolarizing the nerve terminals.

Extracellular Ca^{2+} is required for vesicle fusion and neurotransmitter release at the presynaptic membrane. Omission of Ca^{2+} from ACSF bathing the slice reduced the fluorescence induced by electrical stimulation 76% and by 50 mM K^+ 73% (Fig. 3*E*). Blockade of N-type voltage-gated calcium channels, which are known to play a key role in the entry of calcium into presynaptic nerve terminals during synaptic transmission (Wheeler et al. 1994), by ω-conotoxin GVIA (5 μM), also reduced Zn^{2+} release (by 56 $\pm$ 11%, $n = 5$). These findings indicate that Zn^{2+} is stored in presynaptic vesicles that are released by an exocytotic process triggered by influx of Ca^{2+} via N-type calcium channels following depolarization of the nerve terminal.

To determine whether Zn^{2+} enters postsynaptic neurons under physiologically relevant conditions, we loaded slices with cell-permeable NG diacetate to monitor changes in intracellular Zn^{2+} concentration. Unlike the cell-permeable dye TSQ, which can pass through vesicular membranes, the membrane-permeable ester of NG does not bind vesicular Zn^{2+} in situ, presumably because it is hydrolyzed in the bouton cytosol before it can penetrate vesicles. When electrical stimulation was applied to the mossy fibers, an immediate increase in intracellular fluorescence was observed (Fig. 4, *A–C*). We saw similar increases of fluorescence intensity in the hilar region

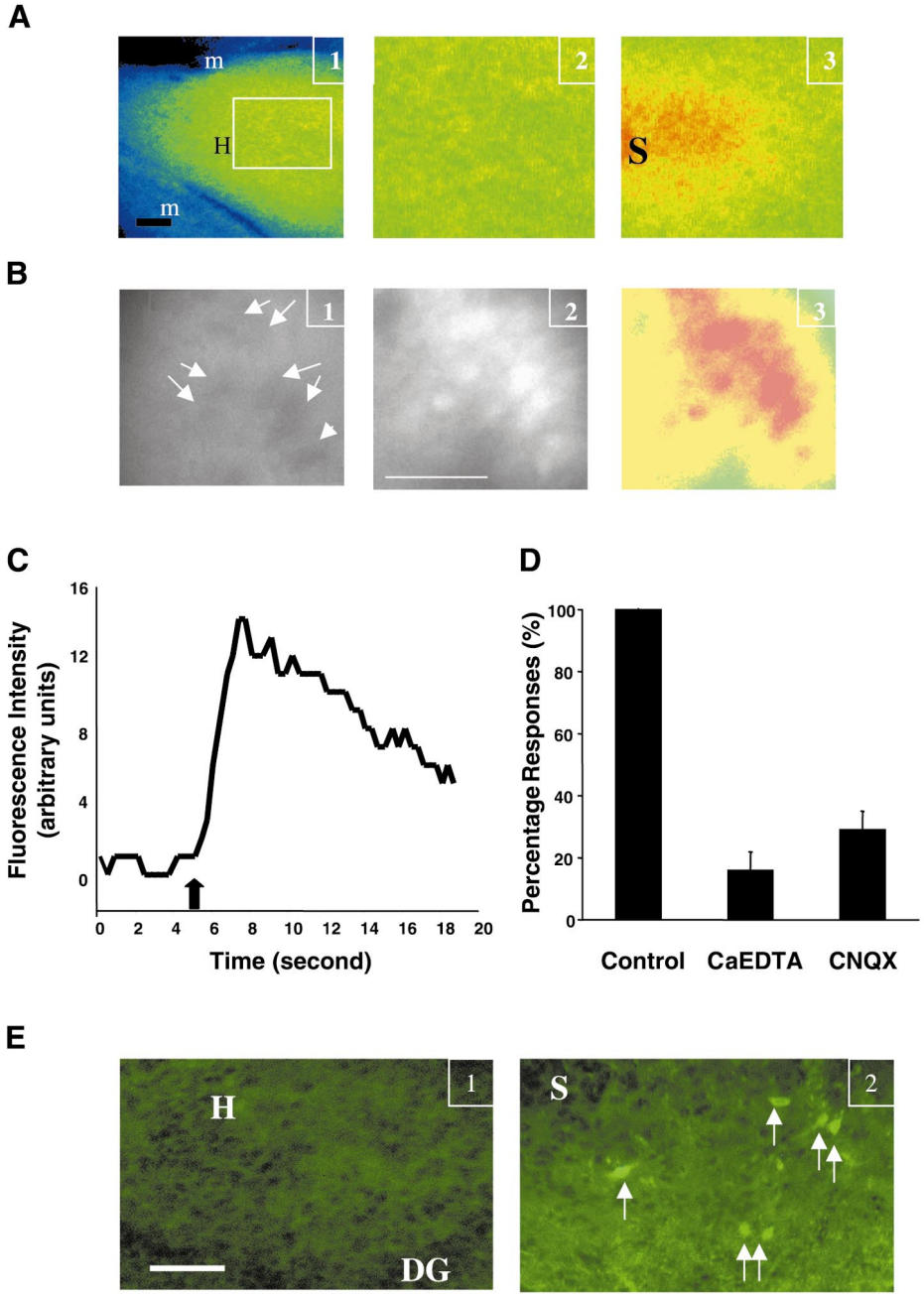

FIG. 4. Influx of presynaptically released Zn^{2+} into postsynaptic neuron. *A*: a typical image (*1*) of the dentate hilus region loaded with NG diacetate. The square region in the hilus is enlarged (*2*) and shows an increase in NG fluorescence (*3*) after electrical stimulation (100 Hz for 10 s). Bar represents 100 μm. m, molecular layer of DG. *B*: images of the pyramidal layer of CA3 taken with a $\times$63 objective lens. Before stimulation (*1*), no cell bodies were labeled; they became visible (*2*) after stimulation (100 Hz for 10 s). *B3* is the same as *B2* but with a pseudocolor scale. Bar represents 50 μm. *C*: electrical stimulation (100 Hz for 10 s) evoked increase of intracellular Zn^{2+}. Arrow indicates the beginning of stimulation. *D*: increase of intracellular Zn^{2+} was depressed in the presence of Zn^{2+} chelator, CaEDTA (10 mM), and an antagonist of AMPA/kainate receptor, CNQX (10 μM). *E*: *N*-(6-methoxy-8-quinolyl)-*p*-toluenesulfonamide (TSQ) staining for 1 min of 2 sample sections of hilus. The section without stimulation (*1*) shows minimum TSQ staining; no cell bodies can be seen. *E2*: after receiving stimulation (500 Hz for 5 s), Zn^{2+}-containing postsynaptic cell bodies (arrows) are visible. S, stimulating electrode. Bar represents 100 μm.

(Fig. 4*A*) and CA3 pyramidal cell layer (Fig. 4*B*). As in our experiments using cell-impermeable NG, the fluorescence from the intracellular dye was also limited to the direction of mossy fiber transmission (data not shown). This increase in intracellular Zn^{2+} fluorescence was not observed when the cell-impermeable Zn^{2+} chelator, CaEDTA (10 mM), was included in the ACSF bathing the slice (Fig. 4*D*, $n = 5$). This indicated that chelation of Zn^{2+} in the extracellular synaptic cleft prevented its entry into the postsynaptic neuron, where it encountered the intracellular dye. CaEDTA was added 5–10 min before the stimulation of slices preloaded with cell-permeable NG. We did not detect any change in the baseline NG fluorescence during the 20 min that we recorded. The increase of intracellular Zn^{2+} after electrical stimulation was also inhibited by an antagonist of AMPA/kainate receptor, CNQX (10 μM) (Fig. 4*D*, $n = 5$). The blockade of AMPA/kainate receptors has been shown to block Zn^{2+} entry into cultured neurons (Sensi et al. 1999; Weiss and Sensi 2000). In slices ($n = 4$) stimulated to produce maximal Zn^{2+} entry into postsynaptic neurons (hilar interneurons and CA3 pyramidal cells) and stained for Zn^{2+} by TSQ, we also found a clear increase in the number of cell bodies that stained for Zn^{2+} along the mossy fiber pathway (Fig. 4*E*). These observations provide direct evidence of Zn^{2+} influx into postsynaptic neurons after its release from presynaptic terminals.

DISCUSSION

In this study, we directly demonstrate that Zn^{2+}-containing neurons release Zn^{2+} immediately from synaptic terminals into the extracellular microenvironment during brief trains of electrical stimulation. Furthermore, we provide the first characterization of the release of Zn^{2+} from synaptic terminals. Zn^{2+} release is stimulation frequency dependent and confined to stimulated axon pathways. Like the release of neurotransmitters, the release of Zn^{2+} is Ca^{2+} dependent and is TTX sensitive. However, unlike conventional neurotransmitters, Zn^{2+}, once released, enters postsynaptic neurons. Our results suggest that Zn^{2+} may also function uniquely as a synaptically released second messenger.

To observe Zn^{2+} release from neuronal terminals directly, it is necessary to employ a cell-impermeable Zn^{2+} fluorescent indicator. Unlike Ca^{2+}, Zn^{2+} has few selective fluorescence indicators available. Several fluorescence probes have been used for detecting movement of Zn^{2+}. However, either toxicity (such as TSQ) or sensitivity to calcium and magnesium (such as Mag-fura-5 and Mag-fura-2) has limited them as effective tools for Zn^{2+} detection. Recently, a carbonic anhydrase-based biosensor system (ABD-N) was used to detect extracellular Zn^{2+} (Thompson et al. 2000). Anticipating that released Zn^{2+} might saturate this dye (K_d for ABD-N for $Zn^{2+} = 4$ pM), we turned to NG, a newly synthesized low-affinity dye.

NG offers several advantages for fluorescence imaging studies of the release of vesicular Zn^{2+}. First, it is very selective for Zn^{2+}. We found that NG fluorescence was not appreciable in the presence of 10 mM Ca^{2+} and Mg^{2+}. This was essential for the detection of synaptically released Zn^{2+} in extracellular medium (ACSF). Second, it is available in cell-permeable and -impermeable forms. Third, its relatively low-affinity makes NG especially useful for detecting high concentrations of extracellular Zn^{2+} released from terminals. Fourth, unlike TSQ, the membrane-permeable ester of NG does not bind vesicular Zn^{2+}. This feature allowed us to measure rapid translocation of Zn^{2+} released from synaptic terminals into postsynaptic cells.

We estimated, using the method by Grynkiewicz et al. (1985), that about 12 μM Zn^{2+} was released by the electrical stimulation used in these experiments. This is probably an underestimation of the actual concentration in the synaptic cleft because we estimated the average fluorescence within an ROI, and the synaptic cleft comprised only a fraction of the extracellular space in that ROI. Using the known sensitivity of the electrophysiological signal of the NMDA receptor to Zn^{2+}, Vogt et al. (2000) estimated that the Zn^{2+} present in the synaptic cleft during an electrical stimulation paradigm similar to ours is between 10 μM and 100 μM.

We conclude that Zn^{2+}-containing neurons release Zn^{2+} into the synaptic cleft when physiologically active and that the released Zn^{2+} attains sufficient concentrations both to modulate known Zn^{2+}-sensitive postsynaptic receptors and to enter postsynaptic neurons. The fluorescent signal we observed most likely represented the release of Zn^{2+} because NG is selective for Zn^{2+} and because similar release from organotypic cultures was observed using another Zn^{2+}-selective probe carbonic anhydrase-ABD-N (Thompson et al. 2000). This is consistent with evidence that virtually all free or weakly bound Zn^{2+} present in normal brain is located in presynaptic vesicles. The colocalization of Zn^{2+} and glutamate implies that Zn^{2+} is involved in the function of the glutamatergic synapses. Work on cultured neocortical or hippocampal neurons has indicated that Zn^{2+}

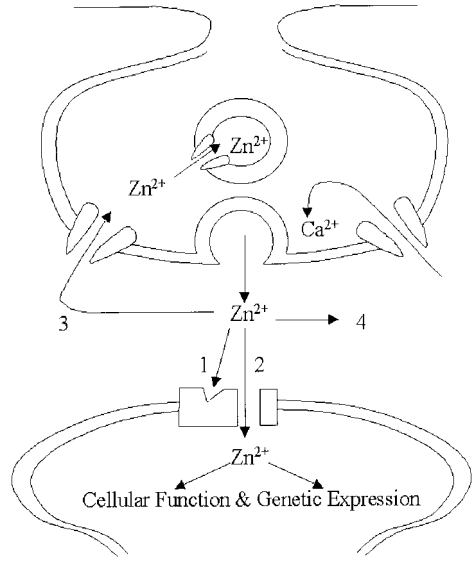

FIG. 5. Schematic illustration of Zn^{2+} containing bouton and postsynaptic neuron indicating Zn^{2+} movements after its release. 1 and 2: following its Ca^{2+}-dependent release, Zn^{2+} can both modulate postsynaptic receptor function (Fisher and Macdonald 1998; Lu et al. 2000; Peters et al. 1987; Smart et al. 1994; Vogt et al. 2000; Westbrook and Mayer 1987) and enter postsynaptic neurons (Sensi et al. 1999). 3: Zn^{2+} can be taken up into the presynaptic terminal and vesicles (Colvin 1998; Howell et al. 1984; Palmiter et al. 1996). 4: finally, released Zn^{2+} can diffuse away into extracellular fluid and be captured by enzymes such as carbonic anhydrase II (Lindskog and Coleman 1973; Thompson et al. 2000).

inhibits NMDA receptors (NMDARs) through two mechanisms (Chen et al. 1997; Choi and Lipton 1999): a high-affinity voltage-independent inhibition, as well as a low-affinity voltage-dependent inhibition, of NMDAR function.

Our data support the notion that Zn^{2+} can be co-released with glutamate and can enter postsynaptic neurons by penetrating several different channels that are gated by membrane voltage and/or glutamate (Sensi et al. 1999) that were blocked in the presence of CNQX (Fig. 4*C*). Thus Zn^{2+} translocation into postsynaptic neurons would not occur unless both presynaptic release and postsynaptic channel opening occurred simultaneously. There is a possibility that synaptically released Zn^{2+} could be taken up into glia and presynaptic terminals (but not vesicles directly), which may add to the residual signal seen in the presence of CNQX. A small amount may also enter neurons through NMDA receptors and VDCC active at the resting membrane potential. The present results indicate that a major portion of the intracellular NG fluorescence is due to synaptically released Zn^{2+} entering postsynaptic neurons in the mossy fiber pathway. Further experiments with various pharmacological agents will help to fully understand the mechanism of Zn^{2+} entry into postsynaptic neurons. Because it evidently acts as both a *trans*-synaptic and a transmembrane signal, Zn^{2+} may rival Ca^{2+} in the diversity of its actions. Our results suggest that Zn^{2+} may function uniquely as a synaptically released second messenger. Intracellular Zn^{2+} is known to affect a number of signal transduction pathways, such as those mediated by Erk 1/2 (Park and Koh 1999), protein kinase C (PKC) (Hubbard et al. 1991) and calmodulin (Brewer et al. 1979). The fact that Zn^{2+}-containing axonal boutons are preferentially concentrated in hippocampus, amygdala, and cerebral cortex, where synaptic plasticity is robust, suggests to us that Zn^{2+} may play an important role in development and experiential learning.

In summary, the characterization of Zn^{2+} release with electrical stimulation has revealed compelling evidence that Zn^{2+}, like neurotransmitters, could be released from synaptic terminals. These data are consistent with storage of Zn^{2+} in synaptic vesicles and release under the same conditions that cause the release of neurotransmitters. To our knowledge, Zn^{2+} is the only messenger substance that is released presynaptically and moves relatively freely into postsynaptic neurons (Fig. 5).

We thank Dr. Richard Thompson for helpful discussion and encouragement throughout this study and B. Cox for comments on the manuscript. Y. Li and J. M. Sarvey thank Dr. Paul Lea for support in managing the laboratory.

This research was supported by grants from the Brain Injury Association and the National Institute of Neurological Disorders and Stroke (NINDS; NS-23865) to J. M. Sarvey and generous support from Theodore and Vada Stanley to C. J. Hough. This work was also supported in part by NINDS Grants NS-40215 and NS-38585 to C. J. Frederickson. The opinions and assertions contained herein are the private opinions of the authors and are not to be construed as official or reflecting the views of the Uniformed Services University of the Health Sciences or the U.S. Department of Defense.

REFERENCES

ANIKSZTEJN L, CHARTON G, AND BEN-ARI Y. Selective release of endogenous zinc from the hippocampal mossy fibers in situ. *Brain Res* 404: 58–64, 1987.

ASSAF SY AND CHUNG SH. Release of endogenous Zn^{2+} from brain tissue during activity. *Nature* 308: 734–736, 1984.

BREWER GJ, ASTER JC, KNUTSEN CA, AND KRUCKEBERG WC. Zinc inhibition of calmodulin: a proposed molecular mechanism of zinc action on cellular functions. *Am J Hematol* 7: 53–60, 1979.

CANZONIERO LM, TURETSKY DM, AND CHOI DW. Measurement of intracellular free zinc concentrations accompanying zinc-induced neuronal death. *J Neurosci* (Online) 19: RC31, 1999.

CHEN N, MOSHAVER A, AND RAYMOND LA. Differential sensitivity of recombinant N-methyl-D-aspartate receptor subtypes to zinc inhibition. *Mol Pharmacol* 51: 1015–1023, 1997.

CHOI YB AND LIPTON SA. Identification and mechanism of action of two histidine residues underlying high-affinity Zn^{2+} inhibition of the NMDA receptor. *Neuron* 23: 171–180, 1999.

COLVIN RA. Characterization of a plasma membrane zinc transporter in rat brain. *Neurosci Lett* 247: 147–150, 1998.

FISHER JL AND MACDONALD RL. The role of an alpha subtype M2–M3 His in regulating inhibition of GABAA receptor current by zinc and other divalent cations. *J Neurosci* 18: 2944–2953, 1998.

FREDERICKSON CJ, KASARSKIS EJ, RINGO D, AND FREDERICKSON RE. A quinoline fluorescence method for visualizing and assaying the histochemically reactive zinc (bouton zinc) in the brain. *J Neurosci Methods* 20: 91–103, 1987.

FREDERICKSON CJ, KLITENICK MA, MANTON WI, AND KIRKPATRICK JB. Cytoarchitectonic distribution of zinc in the hippocampus of man and the rat. *Brain Res* 273: 335–339, 1983.

FREDERICKSON CJ, SUH SW, SILVA D, AND THOMPSON RB. Importance of zinc in the central nervous system: the zinc-containing neuron. *J Nutr* 130: 1471S–1483S, 2000.

GRYNKIEWICZ G, POENIE M, AND TSIEN RY. A new generation of Ca^{2+} indicators with greatly improved fluorescence properties. *J Biol Chem* 260: 3440–3450, 1985.

HAUG FM. Electron microscopical localization of the zinc in hippocampal mossy fibre synapses by a modified sulfide silver procedure. *Histochemie* 8: 355–368, 1967.

HAUGLAND HP. *Handbook of Fluorescent Probes and Research Chemicals* (6th ed.). Eugene, OR: Molecular Probes, 1996.

HOWELL GA, WELCH MG, AND FREDERICKSON CJ. Stimulation-induced uptake and release of zinc in hippocampal slices. *Nature* 308: 736–738, 1984.

HUBBARD SR, BISHOP WR, KIRSCHMEIER P, GEORGE SJ, CRAMER SP, AND HENDRICKSON WA. Identification and characterization of zinc binding sites in protein kinase C. *Science* 254: 1776–1779, 1991.

KOH JY AND CHOI DW. Zinc toxicity on cultured cortical neurons: involvement of N-methyl-D-aspartate receptors. *Neuroscience* 60: 1049–1057, 1994.

LINDSKOG S AND COLEMAN JE. The catalytic mechanism of carbonic anhydrase. *Proc Natl Acad Sci USA* 70: 2505–2508, 1973.

LU Y, TAVERNA FA, TU R, ACKERLEY CA, WANG Y-T, AND RODER J. Endogenous Zn^{2+} is required for the induction of long-term potentiation (LTP) at rat hippocampal mossy fiber-CA3 synapses. *Synapses* 38: 187–197, 2000.

PALMITER RD, COLE TB, QUAIFE CJ, AND FINDLEY SD. ZnT-3, a putative transporter of zinc into synaptic vesicles. *Proc Natl Acad Sci USA* 93: 14934–14939, 1996.

PARK JA AND KOH JY. Induction of an immediate early gene egr-1 by zinc through extracellular signal-regulated kinase activation in cortical culture: its role in zinc-induced neuronal death. *J Neurochem* 73: 450–456, 1999.

PEREZ-CLAUSELL J AND DANSCHER G. Intravesicular localization of zinc in rat telencephalic boutons. A histochemical study. *Brain Res* 337: 91–98, 1985.

PEREZ-CLAUSELL J AND DANSCHER G. Release of zinc sulphide accumulations into synaptic clefts after in vivo injection of sodium sulphide. *Brain Res* 362: 358–361, 1986.

PETERS S, KOH J, AND CHOI DW. Zinc selectively blocks the action of N-methyl-D-aspartate on cortical neurons. *Science* 236: 589–593, 1987.

SARVEY JM, BURGARD EC, AND DECKER G. Long-term potentiation: studies in the hippocampal slice. *J Neurosci Methods* 28: 109–124, 1989.

SENSI SL, YIN HZ, CARRIEDO SG, RAO SS, AND WEISS JH. Preferential Zn^{2+} influx through Ca^{2+}-permeable AMPA/kainate channels triggers prolonged mitochondrial superoxide production. *Proc Natl Acad Sci USA* 96: 2414–2419, 1999.

SMART TG, XIE X, AND KRISHEK BJ. Modulation of inhibitory and excitatory amino acid receptor ion channels by zinc. *Prog Neurobiol* 42: 393–341, 1994.

THOMPSON RB, WHETSELL WO JR, MALIWAL BP, FIERKE CA, AND FREDERICKSON

CJ. Fluorescence microscopy of stimulated Zn(II) release from organotypic cultures of mammalian hippocampus using a carbonic anhydrase-based biosensor system. *J Neurosci Methods* 96: 35–45, 2000,

VOGT K, MELLOR J, TONG G, AND NICOLL R. The actions of synaptically released zinc at hippocampal mossy fiber synapses. *Neuron* 26: 187–196, 2000.

WANG YX AND QUASTEL DM. Multiple actions of zinc on transmitter release at mouse end-plates. *Pflügers Arch* 415: 582–587, 1990.

WEISS JH AND SENSI SL. Ca^{2+}-Zn^{2+} permeable AMPA or kainate receptors: possible key factors in selective neurodegeneration. *Trends Neurosci* 23: 365–371, 2000.

WESTBROOK GL AND MAYER ML. Micromolar concentrations of Zn^{2+} antagonize NMDA and GABA responses of hippocampal neurons. *Nature* 328: 640–643, 1987.

WESTERGAARD N, BANKE T, WAHL P, SONNEWALD U, AND SCHOUSBOE A. Citrate modulates the regulation by Zn^{2+} of N-methyl-D-aspartate receptor-mediated channel current and neurotransmitter release. *Proc Natl Acad Sci USA* 92: 3367–3370, 1995.

WHEELER DB, RANDALL A, AND TSIEN RW. Roles of N-type and Q-type Ca^{2+} channels in supporting hippocampal synaptic transmission. *Science* 264: 107–111, 1994.